INTEGRATION OF SAR AND GEOBIA FOR THE ANALYSIS OF TIME-SERIES DATA

D. Amitrano [a], F. Cecinati [b], G. Di Martino [a], A. Iodice [a], P.-P. Mathieu [c], D. Riccio [a], G. Ruello [a]

[a] University of Napoli Federico II, Napoli, Italy
[b] University of Bath, Bath, UK
[c] European Space Agency, ESA ESRIN, Frascati, Italy

ABSTRACT

In this work, we present a new architecture for the analysis multitemporal SAR data combining classic synthetic aperture radar processing and geographical object-based image analysis. The architecture exploits the characteristics of the recently introduced RGB products of the Level-1α and Level-1β families, employing self-organizing map clustering and object-based image analysis aiming at the definition of opportune layers measuring scattering and geometric properties of candidate objects to classify. The obtained results have been compared with those given by literature and turned out to provide high degree of accuracy and negligible false alarms. The discussion is supported by an example concerning small reservoir mapping in semi-arid environment.

Index Terms— multitemporal synthetic aperture radar, classification, self-organizing map clustering, object-based image analysis

1. INTRODUCTION

Earth observation exploitation in applications is today rather limited, because it requires to end-users, who usually prefer to work in GIS environments, to handle sophisticated data analysis algorithms. This is especially true for SAR data, which are largely underused due to the high expertise required for their handling. Therefore, the development of new tools for satellite data management, integrating remote sensing and GIS technologies, is the key for enlarging the user community.

To this end, many authors suggest to balance perceptive insights and mathematics for creating end-user-oriented frameworks [1, 2], also introducing the concept of geographical object-based image analysis (GEOBIA) [3]. This approach aims at extracting information from remote sensing data by mimicking the way in which humans visually interpret images.

The crucial step for applying OBIA to remote sensing images is the object definition. This is typically done through segmentation, obtaining good results with optical data. Dealing with SAR, this approach can not be replicated as is, because the speckle hampers segmentation and semantics extraction from images. Accordingly, common practice in SAR data processing is to focus the innovation on information extraction algorithms.

In this work, we introduction a novel architecture for feature extraction aiming at the extension of GEOBIA to SAR time series. The goal is the creation of a bridge between GEOBIA and SAR communities, providing easy-to-use tools for data exploitation. We start from well-established methods, as self-organizing map clustering (SOM, see Figure 1) [4] and OBIA [5], and exploit the characteristics of the the recently introduced products of the Level-1α and Level-1β families [2, 6, 7]. These products constitute the input for a SOM clustering. Within the cluster map, those more relevant with the feature of interest are selected, using colors as discriminant, to build a pre-classification mask. This mask is then analyzed with an application-oriented OBIA in which opportune object-layers are defined to classify.

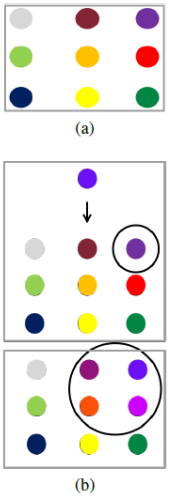

Fig. 1. (a) Initial, randomly initialized SOM. (b) The BMU and its neighbor are updated to become more similar to the presented training set.

The work is organized as follows. Examples of SOM clustering application to multitemporal SAR images are provided in Section 2. OBIA is discussed in an application-oriented

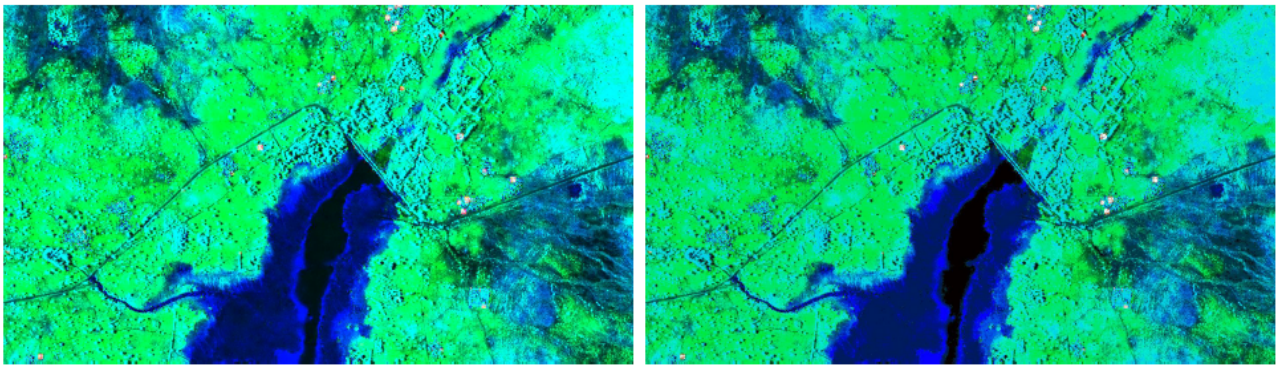

(a) (b)

Fig. 2. Burkina Faso dataset. (a) Sample Level-1α RGB product and (b) its 49-cluster version obtained through SOM clustering. Each cluster is associated to a color label.

environment in Section 3, where we address the problem of small reservoir mapping in semi-arid environment. Conclusions are drawn at the end of the work.

2. APPLICATION OF SOM CLUSTERING TO MULTITEMPORAL SAR IMAGES

SOM, is a machine-learning technique of the artificial neural network family. Its principle is schematized in Figure 1, in which nodes are constituted by RGB triplets. In the classic Kohonen's schema [4], they are randomly initialized (Figure 1a) and connected by a rectangular structure. The nodes are trained using a pre-determined number of sample vectors randomly selected from the input data. Each time a training vector is compared to the SOM, the most similar node is detected. It represents the best matching unit (BMU, see Figure 1b). The BMU and its neighbor are updated to become more similar to the presented training sample. This operation is repeated for several iterations. After many iterations, the SOM becomes stable, and the obtained nodes can be used to classify data.

In Figure 2, we show an example of the application of SOM clustering to a multitemporal RGB Level-1α product [2]. In particular, in Figure 2a, a Level-1α product concerning a rural area in Burkina Faso (western Africa) is shown. The image has been built placing an image acquired during the dry season on the blue band (it represent the reference image); on the green band, there is an image acquired during the wet season (representing the test acquisition); the red band is reserved to the interferometric coherence, and it is useful to identify small human settlements because they are stable with respect to phase. As stated in [2], this composition allows for displaying seasonal water in blue color.

In Figure 2b, we show the 49-cluster SOM version of the input product. It is remarkable that SOM outputs a cluster map that is very similar to the input product. This allows for an immediate semantic transfer from one image to the other. In other words, it is possible to associate, as an example, clusters with dominant green color to vegetation and those with dominant blue to water. This allows for easily identify a pre-classification mask relevant with the feature of interest. This is possible exploiting the color label that is automatically attached to each output cluster. In the next section, we will show how to extract small reservoirs starting from this mask extracted from the cluster map.

3. APPLICATION-ORIENTED OBIA FOR SMALL RESERVOIRS MAPPING IN SEMI-ARID ENVIRONMENT

In semi-arid environment, small reservoirs are a fundamental resource for facing water scarcity during dry seasons. Their monitoring is crucial for the wellness of local population. In this contexts, remote sensing is very helpful, providing up-to-date information with high temporal and spatial resolution in areas otherwise scarcely monitored [8].

To this end, the processing chain depicted in Figure 3 is proposed. The pre-classification mask, obtained by selecting the clusters relevant with water using the colors displayed in the cluster map, is analyzed using two opportune object-layers, one scattering-based, the other geometry-based. The scattering layer is given by the mean (computed object-wise) of the seasonal water pseudo-probability (SWPP) [9]. It is an index measuring the pseudo-probability that a pixel is covered by seasonal water, which is computed as follows:

$$\text{SWPP} = \left[1 - \left(\frac{G}{255}\right)^2\right] \frac{B-G}{B+G}, \qquad \text{SWPP} \in [-1, 1]\,. \tag{1}$$

In this formula, B and G are the blue and the green band of a Level-1α product, respectively. Roughly, it allows for having a high response in areas where the blue color appears

in the RGB product. For further details, the reader can refer to [9].

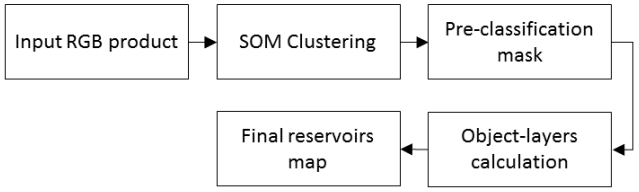

Fig. 3. OBIA chain for small reservoirs mapping.

The geometric layer is represented by the compactness, which basically measures how much an object is shaped like a circle. It is a very consolidated shape index in image understanding problems, and it is computed as follows [10]:

$$\mathrm{C} = \frac{4\pi A}{P^2}, \quad \mathrm{C} \in]0, 1]. \tag{2}$$

In this formula, A and P represent objects' area and perimeter, respectively. For a circle, the compactness is equal to one. However, in the digital world, it is impossible to have a circle. Therefore, in this case, the most compact object is the square, for which the compactness is about 0.78.

Objects having the scattering and geometric properties compatible with those of a reservoir (high SWPP and high compactness) are selected through a fuzzy system able to assign the final classes "reservoir"/"no reservoir" without supervision through the maximum membership criterion [11].

The results of the application of this approach to six images of our Burkina Faso dataset acquired between 2010 and 2014 are reported in Table 1. In the same table, we also reported the results obtained by applying literature method like thresholding of the SWPP map, maximum likelihood (ML), and support vector machine (SVM) classifications. Notice that ML and SVM are supervised method, therefore relevant training samples have been selected for each class of interest and for each analyzed image. Both pixel-based and object-based performance parameters (overall accuracy and false alarms) have been considered.

From this table, it arises that the proposed methodology allows for obtaining the best trade-off between overall accuracy and false alarms. In fact, on average, the registered overall accuracy for the proposed method is 85.8%. For the other methods we had: SWPP - 91.5%, ML - 91.2%, SVM - 87.2%. Therefore, our method registered just few point less of accuracy with respect to the best registered performance (that is the one of SWPP classification).

On the other hand, a significant improvement is obtained concerning false alarms. As an example, if we consider the ML classification, having good performance in terms of accuracy, we have at least two classifications completely failed (2014/07/01 and 2014/08/26) despite an expert selection of training samples. For the SWPP, we have 9 false objects, on average, per image classified. As for the SVM, the registered average for false reservoirs is about 6. The proposed methodology obtained the best result, with an average of one false object per classification.

The analysis of the results reported in Table 1 led to the following considerations:

- The proposed (object-based) method has performance comparable to those of literature pixel-based techniques in terms of overall accuracy;
- The introduction of OBIA and its integration with SAR processing allowed for obtaining significant improvement on the false alarm quality parameter. This is very important in the analysis of huge time series of data, where human supervision is necessarily limited;
- The proposed methodology, being fully unsupervised, avoids the selection of relevant training samples for each class of interest and for each image to be analyzed, as in the case of the most common classifiers (such as ML and SVM).

Summarizing, the introduction of OBIA in SAR processing allows for improve the robustness to false alarms in time series analysis, keeping a detection accuracy comparable with that of popular pixel based methods. Moreover, the lack of any supervision makes our method very attractive for the analysis of long time series.

4. CONCLUSIONS

In this work, we presented a novel framework for feature extraction from multitemporal SAR data mixing classic SAR processing and GEOBIA concepts. The proposed innovation was based on the usage of products of the Level-1α and Level-1β families. They were treated with self-organized map clustering allowing for building a pre-classification mask whose objects were analyzed with an application-oriented object-based image analysis to classify.

In particular, two object-layers have been introduced to individuate, among them, those having the scattering and geometric characteristics compatible with those of a reservoir. They were the mean (computed object-wise) of the seasonal water pseudo-probability (scattering layer) and the compactness (geometric layer). A fuzzy system rules the selection/rejection of candidate objects, assigning the class "reservoir"/"no reservoir" automatically through the maximum membership criterion.

The performance of the proposed methodology has been compared with that of popular pixel-based supervised classifiers. As a result, using our method we registered a significant improvement of the robustness to false alarms, keeping a comparable detection accuracy. Moreover, our method, being fully unsupervised, allows for avoiding the selection of relevant training samples for the feature of interest. This is very

Table 1. Comparison between the proposed algorithm and other popular classification methods: seasonal water pseudo-probability (SWPP), maximum likelihood (ML), support vector machine (SVM). N: applied threshold for binary segmentation or number of clusters/classes for supervised classifiers. OA: overall accuracy, FA: false alarm rate. P: pixel-based assessment. O: object-based assessment. Bold characters indicate the best registered performance.

Date	Method	N	OA		FA		Date	Method	N	OA		FA	
			P (%)	O	P $\times E^{-4}$	O				P (%)	O	P $\times E^{-4}$	O
	Proposed	64	90.2	9/9	1.14	2		Proposed	64	85.0	11/11	**0.24**	0
	SWPP	0.3	**94.9**	9/9	3.04	20		SWPP	0.3	**89.5**	11/11	0.47	2
2010/07/14	ML	4	94.4	9/9	1.38	5	2011/10/09	ML	4	78.8	11/11	3.50	40
	SVM	4	92.4	9/9	**1.18**	5		SVM	4	85.8	11/11	0.33	2
	Proposed	64	83.4	13/13	**0.35**	2		Proposed	64	89.0	8/8	**2.70**	2
	SWPP	0.3	**89.8**	13/13	1.35	12		SWPP	0.3	91.8	8/8	4.45	12
2010/08/31	ML	4	89.3	13/13	0.95	8	2014/07/01	ML	4	**98.3**	8/8	594	2069
	SVM	4	88.4	13/13	0.18	3		SVM	4	89.8	8/8	5.87	21
	Proposed	64	84.9	13/13	**0.38**	0		Proposed	64	82.0	9/10	0.71	0
	SWPP	0.3	**90.2**	13/13	0.76	3		SWPP	0.3	92.8	10/10	1.38	5
2010/09/16	ML	4	**90.2**	13/13	1.60	3	2014/08/26	ML	4	**96.4**	10/10	22.4	122
	SVM	4	78.6	13/13	0.43	1		SVM	4	87.9	10/10	**0.70**	2

important in the optic of the analysis of long time series of data, where the human supervision is necessarily limited by the quantity of images to be classified.

5. ACKNOWLEDGMENTS

The authors thank the Italian Space Agency (ASI) for providing the dataset used in this study under the aegis of the "HydroCIDOT" project.

6. REFERENCES

[1] M. Datcu and K. Seidel, "Human-Centered Concepts for Exploration and Understanding of Earth Observation Images," *IEEE Trans. Geosci. Remote Sens.*, vol. 43, no. 3, pp. 52–59, 2005.

[2] D. Amitrano, G. Di Martino, A. Iodice, D. Riccio, and G. Ruello, "A New Framework for SAR Multitemporal Data RGB Representation: Rationale and Products," *IEEE Trans. Geosci. Remote Sens.*, vol. 53, no. 1, pp. 117–133, 2015.

[3] G. J. Hay and G. Castilla, *Geographic Object-Based Image Analysis (GEOBIA): A new name for a new discipline*. Berlin, Heidelberg: Springer, 2008, pp. 75–89.

[4] T. Kohonen, *Self-Organizing Maps*. Berlin, Heidelberg: Springer-Verlag, 2001.

[5] T. Blaschke, "Object based image analysis for remote sensing," *ISPRS J. Photogramm. Remote Sens.*, vol. 65, no. 1, pp. 2–16, 2010.

[6] D. Amitrano, F. Cecinati, G. Di Martino, A. Iodice, P.-P. Mathieu, D. Riccio, and G. Ruello, "Multitemporal Level-1β Products: Definitions, Interpretation, and Applications," *IEEE Trans. Geosci. Remote Sens.*, vol. 54, no. 11, pp. 6545–6562, 2016.

[7] D. Amitrano, G. Di Martino, A. Iodice, D. Riccio, and G. Ruello, "RGB SAR Products: Methods and Applications," *European Journal of Remote Sensing*, vol. 49, pp. 777–793, 2016.

[8] D. Amitrano, F. Ciervo, G. Di Martino, M. N. Papa, A. Iodice, Y. Koussoube, F. Mitidieri, D. Riccio, and G. Ruello, "Modeling Watershed Response in Semi-arid Regions with High Resolution Synthetic Aperture Radars," *IEEE J. Sel. Topics Appl. Earth Observ.*, vol. 7, no. 7, pp. 2732–2745, 2014.

[9] D. Amitrano, G. Di Martino, A. Iodice, , D. Riccio, and G. Ruello, "Small Reservoirs Extraction in Semi-Arid Regions Using Multitemporal Synthetic Aperture Radar Images," *IEEE J. Sel. Topics Appl. Earth Observ.*, vol. 10, no. 8, pp. 3482–3492, 2017.

[10] E. P. Cox, "A method of assigning numerical and percentage values to the degree of roundness," *J. Paleontol.*, vol. 1, no. 3, pp. 179–183, 1927.

[11] D. Amitrano, V. Belfiore, F. Cecinati, G. Di Martino, A. Iodice, P.-P. Mathieu, S. Medagli, D. Poreh, D. Riccio, and G. Ruello, "Urban Areas Enhancement in Multitemporal SAR RGB Images Using Adaptive Coherence Window and Texture Information," *IEEE J. Sel. Topics Appl. Earth Observ.*, vol. 9, no. 8, pp. 3740–3752, 2016.